A new short-anoded IGBT with high emission efficiency*

Chen Weizhong(陈伟中)†, Zhang Bo(张波), Li Zehong(李泽宏), Ren Min(任敏), and Li Zhaoji(李肇基)

State Key Laboratory of Electronic Thin Films and Integrated Devices, University of Electronic Science and Technology of China, Chengdu 610054, China

Abstract: A novel short-anoded insulated-gate bipolar transistor (SA-IGBT) with double emitters is proposed. At the on-state, the new structure shows extraordinarily high emission efficiency. Moreover, with a short-contacted anode, it further enhances the hole emission efficiency because of the crowding of the electrons. The forward voltage drop V_F of this structure is 1.74 V at a current density 100 of A/cm^2. Compared to the conventional NPT IGBT (1.94 V), segment-anode IGBT (SA-NPN 2.1 V), and conventional SA-IGBT (2.33 V), V_F decreased by 10%, 17% and 30%, respectively. Furthermore, no NDR has been detected comparing to the SA-IGBT. At the off-state, there is a channel for extracting excessive carriers in the drift region. The turn-off loss E_{off} of this proposed structure is 8.64 mJ/cm^2. Compared to the conventional NPT IGBT (15.3 mJ/cm^2), SA-NPN IGBT (12.8 mJ/cm^2), and SA-IGBT (12.1 mJ/cm^2), E_{off} decreased by 43.7%, 32% and 28%, respectively.

Key words: short-anode insulated-gate bipolar transistor; snapback; turn-off; tradeoff

DOI: 10.1088/1674-4926/33/11/114003 **EEACC:** 2570

1. Introduction

The insulated-gate bipolar transistor (IGBT) is a promising power semiconductor device due to its unique combination of voltage control in MOS devices and conductivity modulation in bipolar devices, which makes it very favorable for medium voltage power applications[1−4]. At the on-state, as compared to the unipolar transistor, many holes are injected in the drift region; this significantly reduces the forward voltage drop V_F of the IGBT. However, at the off-state, there is no channel for extracting the excessive carriers, so it significantly increases the turn-off loss E_{off}. Consequently, many methods such as the transparent anode[5], striped anode[6], DG-IGBT[7] and short-anoded IGBT (SA-IGBT)[8] have been adopted to solve this problem by optimizing the anode; so-called anode engineering[9]. Obviously, SA-IGBT is the most effective way to extract the excessive carriers. However, several drawbacks are observed in the on-state properties. The first is that the V_F of the SA-IGBT is very large because of its lower emission efficiency. Secondly, the device is prone to undesirable snapback (i.e., the negative differential resistance (NDR) region in the forward conduction state). When the devices are paralleled, this deleterious effect can prevent their full turn-on, especially at low temperature. Subsequently the segment anode structure (SA-NPN) with a p-base was proposed[10−13] for suppressing the NDR. Even though it has higher emission efficiency than the SA-IGBT, it is still inferior to the conventional IGBT, and leads to a higher E_{off}.

In this letter, a new SA-IGBT with double emitters and short-contacted anode is presented to enhance the emission efficiency at the on-state, and extract the excessive carriers as the SA-IGBT at the turn-off process, and eventually offer better trade-off properties.

2. Structure and mechanism

2.1. Proposed structure

A schematic cross section of the proposed device is illustrated in Fig. 1. Compared to the conventional SA-IGBT, a second anode P_2 is introduced above the metal. On one hand this anode offers a potential barrier to the electrons flowing directly to the metal and consequently increases the anode resistance and voltage in the unipolar mode. On the other hand, as illustrated in the equivalent circuit, another transistor P_2NP enhances hole emission efficiency at the on-state. Moreover, the double SiO_2 layers cause crowding of the electrons near the anode, and further reduce V_F. The narrow channel sandwiched between the double anodes allows extraction of electrons during the turn-off process.

2.2. Theoretical analysis

Equations (1)–(7) show the relationship of the key parameters of the proposed devices for initiating hole injection. At this point, device conduction changes from unipolar to bipolar mode:

$$V_{total} = V_p + V_{others}, \tag{1}$$

$$\begin{aligned} V_p &= I_{MOS} R_{\square}(L_p - L_c) + \int_{Lp}^{L_M} \frac{I_{MOS}}{L_M} x R_{\square} \mathrm{d}x \\ &\quad + \int_0^{L_p} \frac{I_{MOS}}{L_M} x R_{\square} \mathrm{d}x \\ &= \left(\frac{L_a}{2} + L_P\right) I_{MOS} \frac{1}{q N_d \mu_n D_s}. \end{aligned} \tag{2}$$

* Project supported by the National Natural Science Foundation of China (Nos. 60806025, 61076082).

† Corresponding author. Email: cwz@cqu.edu.cn

Received 11 April 2012, revised manuscript received 10 May 2012

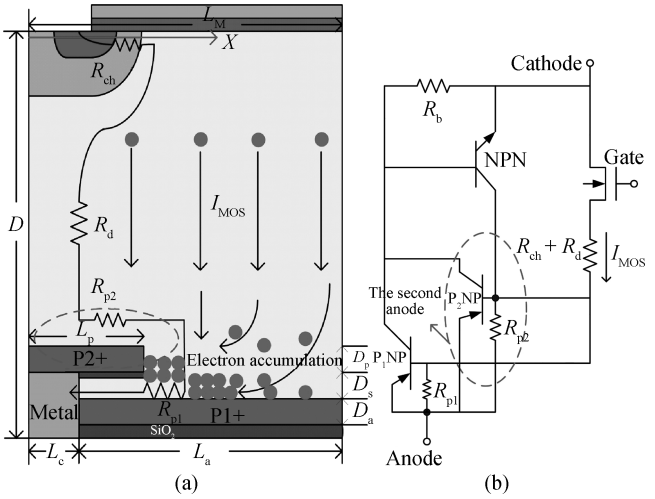

Fig. 1. (a) Schematic cross section of the proposed IGBT. (b) Its equivalent circuit; the dashed circle is the second anode P_2.

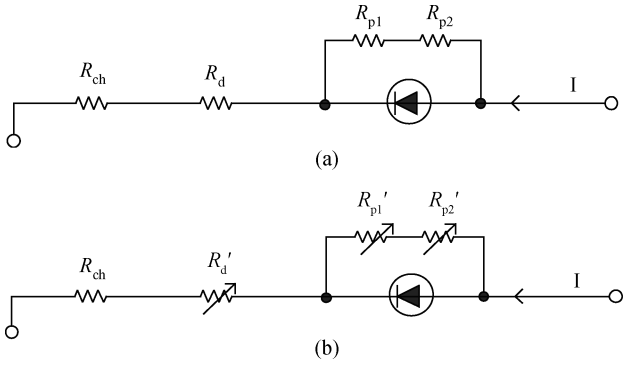

Fig. 2. (a) Snapback point. (b) Holding point.

The extent of the NDR regime as illustrated is determined by the ratio of the drift resistance to the anode resistance[14]. Figure 2 shows the relationship between the resistance at different modes.

Snapback point:

$$V_{SB} = I(R_{ch} + R_d + R_p), \quad I = \frac{0.7}{R_p}, \tag{3}$$

$$V_{SB} = 0.7\left(1 + \frac{R_{ch} + R_d}{R_p}\right). \tag{4}$$

Holding point:

$$V_H \approx V_{SB} - IR_d, \tag{5}$$

$$V_H = V_{SB}\left(1 - \frac{R_d}{R_{ch} + R_d + R_p}\right), \tag{6}$$

$$\Delta V_{SB} = V_{SB} - V_H = 0.7\frac{R_d}{R_p} = \frac{1.4qN_d\mu_n D_s R_d}{L_a + 2L_p}, \tag{7}$$

where V_{total} is the supply voltage; V_p is the anode voltage across the anode resistance R_{p1} and R_{p2}; V_{others} is the voltage across the R_d and R_{ch}; I_{MOS} is the current flow of the MOS channel; $R_\square$ is the sheet resistance along x axis; L_p is the length of the second anode; N_d and D_s are the doping density and width of the narrow electron channel; q is the basic charge; V_{SB} and V_H are the snapback point and holding point respectively; R_d is the resistance of the drift region; R_p is the sum resistance of the R_{p1} and R_{p2}. It can be seen that the anode voltage drop V_p is directly proportional to the second anode length L_p and in the reverse ratio of N_d and D_s. For ΔV_{SB} the situation is just contrary to that for V_p.

Table 1. Device specifications.

Parameter	Proposed	Short-anoded IGBT
Half-MOS cell dimension, L_M (μm)	15	15
Wafer thickness, D (μm)	160	160
N-drift doping, N_B (cm^{-3})	7×10^{13}	7×10^{13}
Anode1 cell length, $L_c + L_a$ (μm)	15	60
Anode1 thickness, D_a (μm)	1	1
Anode1 doping, N_P (cm^{-3})	1×10^{18}	1×10^{18}
Anode1 length, L_a (μm)	14	55
Contact length, L_c (μm)	1	5
Anode2 length, L_p (μm)	1–10	—
Anode2 depth D_p (μm)	1	—
Anode2 doping N_P (cm^{-3})	1×10^{18}	—
Oxide depth, D_{OX} (μm)	0.1	—
Short anode width D_s (μm)	1	—
Trade off variable	L_p	L_c/L_a

For the conventional SA-IGBT, injecting holes depends on the voltage drop across the N-region under anode P_1, where the N-region usually act as an N-buffer; it is difficult for the voltage drop to reach 0.7 V to inject holes from P_1, and it will work as a VDMOS. To solve this problem the usual method is to extend the length of the cell. But for the proposed devices, we can simply lengthen L_p for increasing anode voltage.

3. Results and discussion

In numerical simulations, the proposed and the conventional NPT, SA-NPN, and SA-IGBT have the same structure except for the anode. Key parameter values are listed in Table 1. The thickness and doping concentration of the N-drift region are 160 μm and 7×10^{13} cm^{-3} respectively for a blocking capability of 1200 V. The carrier lifetimes are 1 μs, and the temperature is 25 ℃. In the clamped inductive load (CIL) turn-off simulations, the devices are turned off at forward conduction current density 100 A/cm^2 and line voltage 600 V.

3.1. On-state

Figure 3 shows the numerical simulated I–V characteristics and hole density in the drift region of the conventional NPT, SA-NPN, SA-IGBT, and the proposed IGBT. As seen from Fig. 3(a), at the same current density 100 A/cm^2, the SA-NPN (2.1 V) and the SA-IGBT (2.33 V) have higher forward voltage drop comparing to the conventional NPT IGBT (1.94 V) because of their lower anode emission efficiency. The proposed IGBT, owing to its double emitters and short-contacted anode, has the lowest forward drop (1.74 V), which can decrease by almost 10%, 17%, 30% compared to the other

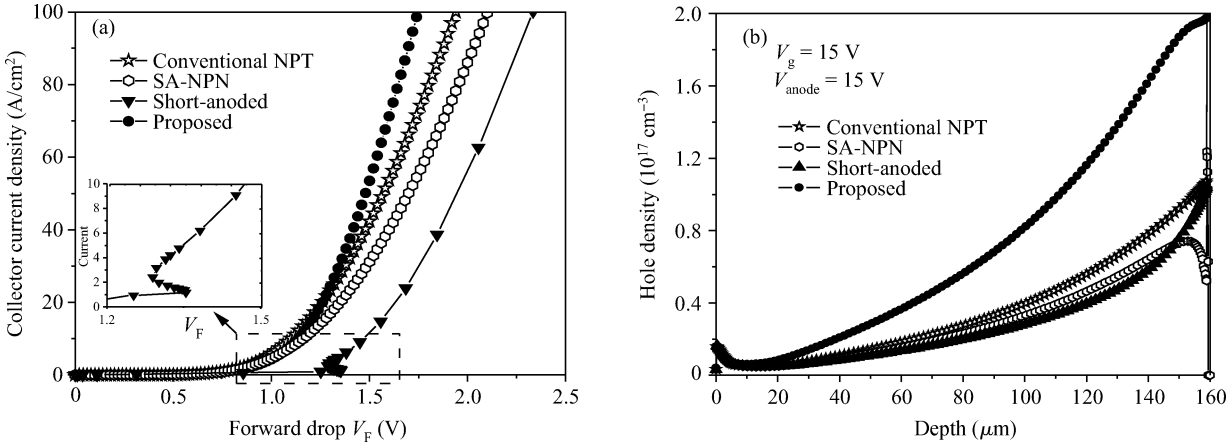

Fig. 3. (a) Forward conduction characteristics of the conventional NPT, SA-NPN, SA-IGBT and proposed IGBT. The p-base doping for the SA-NPN is 1×10^{17} cm^{-3}, the ratio of L_c/L_a for the SA-IGBT is 1 : 11, and the second anode length L_p for the proposed IGBT is 10 μm. (b) Hole density in the drift region of these devices at cut-line $x = 15$ μm when the gate voltage $V_g = 15$ V, anode voltage $V_{anode} = 15$ V.

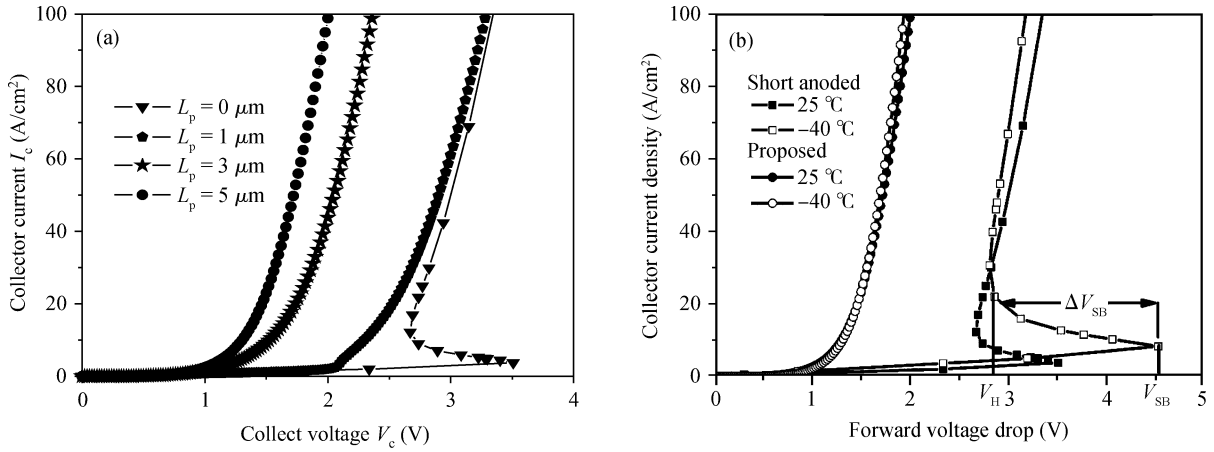

Fig. 4. (a) Dependence of forward conduction characteristics and the length of anode L_p. (b) Dependence of forward conduction characteristics on temperature for the SA-IGBT and proposed IGBT. $\Delta V_{SB} = V_{SB} - V_H$, V_{SB} is the turn-over voltage of snapback. V_H is the holding point.

three devices respectively. Moreover no NDR regime is detected in the I–V characteristics. Figure 3(b) shows the hole density of these devices in the drift region, which further supports the highest emission efficiency of the proposed IGBT.

It is worth noting that for the conventional SA-IGBT, if the ratio L_c/L_a is small enough, the NDR regime can also be eliminated, but it needs either longer L_a or smaller L_c, Both will slow the speed of electron extraction, leading to higher turn-off loss.

Figure 4(a) shows the influences of L_p on the snapback, it can be seen that when $L_p = 1$ μm, there is almost no NDR, Moreover, the V_F decreases rapidly with the longer L_p. Figure 4(b) shows the dependence of forward conduction characteristics on temperature for the SA-IGBT and proposed IGBT. The NDR regime of the SA-IGBT is affected more seriously at lower temperature, but the proposed device shows no snapback even at −40 ℃.

3.2. Switching state

At the same forward voltage drop $V_F = 2.1$ V (the forward current density is 100 A/cm^2), the turn-off current and voltage waveforms are shown in Fig. 5(a). For the proposed structure, the electron channel sandwiched between the double anodes offers a route, as in the conventional SA-IGBT, for extracting excessive carriers. The SA-NPN IGBT depends on the NPN transistor to extract the electrons, which is slower than that of the proposed structure. For the conventional SA-IGBT, although there is a channel for electrons during the turn-off state, it needs a much bigger cell size to attain the same forward voltage drop and suppress the NDR regime. Calculating the turn-off time from 90% I_c to 10% I_c, the proposed IGBT needs 680 ns to turn off. Compared to those of the conventional NPT IGBT (1.1 μs), SA-NPN IGBT (820 ns), SA-IGBT (800 ns), the turn-off time can be decreased by 39%, 17% and 15% respectively. This is attributed to the anode-shortened structure and small anode cell length (four times smaller than that of the conventional SA-IGBT). Figure 5(b) shows the carrier density of the drift region for the three IGBTs at the turn-off process. It can be seen that the proposed IGBT has the best properties for extracting the excessive carriers due to the narrow channel sandwiched between the double emitters.

The trade-off performances between the forward voltage drop and the turn-off loss are comparatively illustrated in Fig. 6. It is obvious that the trade-off curve of the proposed IGBT lies below the others. Ultimately, it achieves the best

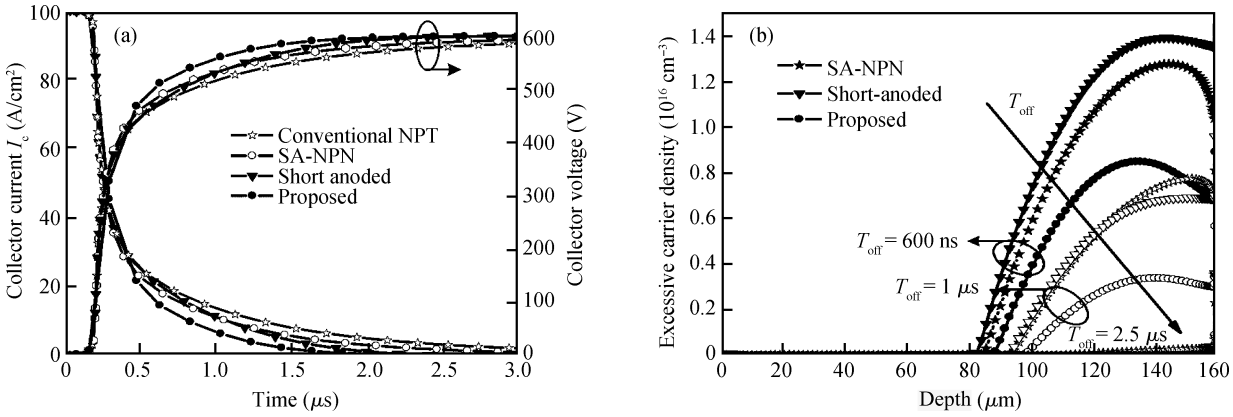

Fig. 5. (a) Turn-off current waveforms and anode voltage waveforms of the conventional NPT IGBT, SA-NPN IGBT, SA-IGBT and the proposed IGBT under a clamped inductive load. $R_g = 10\ \Omega$, $L = 10\ \mu$H, line voltage $V_c = 600$ V; the carrier lifetimes are $t = 1\ \mu$s, and the temperature is $T = 298$ K. (b) The excessive carrier density of the drift region for the three IGBTs at the turn off process when $t_{off} = 600$ ns, $t_{off} = 1\ \mu$s, $t_{off} = 2.5\ \mu$s.

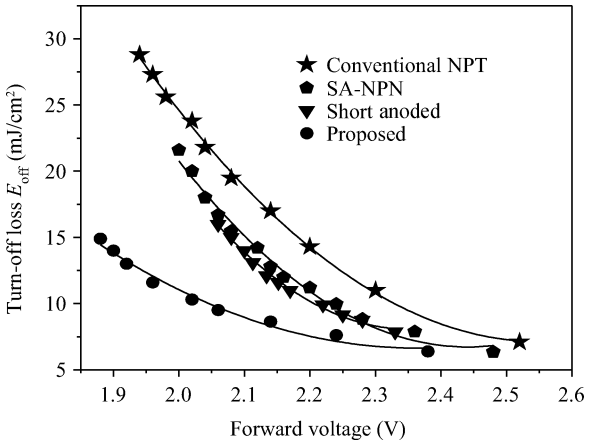

Fig. 6. The trade-off performances between V_F and E_{off} obtained by varying the doping concentrations of the anode for the conventional NPT IGBT, control of the anode p-base region for the SA-NPN IGBT, control of the ration of L_c/L_a for the SA-IGBT, and control of the length of anode2 L_p for the proposed device.

trade-off properties.

4. Conclusion

A short-anoded IGBT with double emitters and short-contacted anode has been presented and investigated by numerical simulations. The new structure shows extraordinarily high emission efficiency and effectively suppresses the NDR region in forward I–V characteristics. Additionally, the electron channel is useful for extracting electrons during the turn-off process. The simulation results show that this structure exhibits the best trade-off properties compared to those of the conventional NPT IGBT, SA-NPN IGBT and SA-IGBT.

References

[1] Uzuka T. Trends in high-speed railways and the implication on power electronics and power devices. Proc 23rd Int Symp Power Semiconductor Devices and IC'S (ISPSD), San Diego, CA, 2011: 6

[2] Yedinak J, Merges J, Wojslawowicz J, et al. Operation of an IGBT in a self-clamped inductive switching circuit (SCIS) for automotive ignition. Proc 10th Int Symp Power Semiconductor Devices and IC'S (ISPSD), Kyoto, Japan,1998: 399

[3] Jiang Huaping, Chen Wanjun, Liu Chuang, et al. Design and optimization of linearly graded-doping junction termination extension for 3.3-kV-class IGBTs. Journal of Semiconductors, 2011, 32(12): 124004

[4] Jiang Huaping, Zhang Bo, Liu Chuang, et al. Experimental study of the anode injection efficiency reduction of 3.3 kV-class NPT-IGBTs due to backside processes. Journal of Semiconductors, 2012, 33(2): 024003

[5] Matsudai T, Tsukuda M, Umekawa S, et al. New anode design concept of 600 V thin wafer PT-IGBT with very low dose P-buffer and transparent P-emitter. IEE Proc Circuits Devices Syst, 2004, 151(3): 255

[6] Luther-King N, Sweet M, Spulber O, et al. Striped anode engineering: a concept for fast switching power devices. Solid-State Electron, 2002, 46(6): 903

[7] Nakagawa A. Numerical experiment for 2500 V double gate bipolar mode MOSFETS (DGIGBT) and analysis for large safe operating area (SOA). Power Electronics Specialists Conf PESC, 1988, 1: 84

[8] Gough A P, Simpson M R, Rumenik V. Fast switching lateral insulated gate transistor. IEEE IEDM Tech Dig, 1986: 218

[9] Green D W, Vershinin K V, Sweet M, et al. Anode engineering for the insulated gate bipolar transistor—a comparative review. IEEE Trans Power Electron, 2007, 22(5): 1857

[10] Green D W, Sweet M, Vershinin K V, et al. Performance analysis of the segment npn anode LIGBT. IEEE Trans Electron Devices, 2005, 52(11): 2482

[11] Hardikar S, Tadikonda R, Sweet M, et al. A fast switching segmented anode npn controlled LIGBT. IEEE Electron Device Lett, 2003, 24: 701

[12] Hardikar S, Xu Y Z, Souza M M D, et al. A segmented anode, npn controlled lateral insulated gate bipolar transistor. Solid-State Electron, 2001, 45: 1055

[13] Chen W, Zhang B, Li Z. Area-efficient fast-speed lateral IGBT with a 3-D n-region-controlled anode. IEEE Electron Device Lett, 2010, 31(5): 467

[14] Antoniou M, Udrea F, Nistor I. The soft punchthrough+ superjunction insulated gate bipolar transistor: a high speed structure with enhanced electron injection. IEEE Trans Electron Devices, 2011, 58(3): 769